

Is there a Granular Potential?

Josh M. Gramlich,^a Mahdi Zarif,^b and Richard K. Bowles^{ac*}

Granular materials, such as sand or grain, exhibit many structural and dynamic characteristics similar to those observed in molecular systems, despite temperature playing no role in their properties. This has led to an effort to develop a statistical mechanics for granular materials that has focused on establishing an equivalent to the microcanonical ensemble and a temperature-like thermodynamic variable. Here, we expand on these ideas by introducing a granular potential into the Edwards ensemble, as an analogue to the chemical potential, and explore its properties using a simple model of a granular system. A simple kinetic Monte Carlo simulation of the model shows the effect of mass transport leading to equilibrium and how this is connected to the redistribution of volume in the system. An exact analytical treatment of the model shows that the compactivity and the ratio of the granular potential to the compactivity determine the equilibrium between two open systems that are able to exchange volume and particles, and that mass moves from high to low values of this ratio. Finally, using the granular potential, we show that adding a particle to the system increases the entropy at high compactivity, but decreases the entropy at low compactivity.

1 Introduction

Macroscopic granular materials, such as sand, grains and dry powders, are jammed systems that remain static unless subject to external forces. When shaken or tapped, the granular particles rearrange, dissipating energy through collisions, before returning to another jammed state. However, when agitated repeatedly, these systems appear to evolve to highly reproducible states in terms of their occupied volume, reminiscent of the type of reproducibility found in thermodynamics^{1,2}. The dynamics of the constituent particles also exhibit properties similar to those observed in molecular systems such as supercooled liquids and glasses^{3,4}, or complex fluids⁵. This has led to the suggestion that the properties of granular materials could be described by an appropriate form of statistical mechanics. As a starting point, Edwards^{6,7} proposed the equivalent to the micro-canonical ensemble by postulating all jammed packings with the same volume are equiprobable, which then defines the entropy as the number of jammed states and the compactivity, a measure of the capacity of the system to be compressed, as the granular equivalent to the thermal temperature. Much of the subsequent work⁸⁻¹⁵ has focused on establishing the validity or otherwise of an appropriate equiprobable ensemble and the equivalent of the zero law of thermodynamics, which defines the nature of equilibrium between systems.

If the properties of granular systems can be described by a form of statistical mechanics, with the compactivity serving as an appropriate temperature-like quantity, it raises the question of whether there are additional granular analogies to the thermodynamic potentials used in chemical systems. The chemical potential plays a central role in our understanding of equilibrium and mass transport in molecular systems. It also provides the basis for many ensembles in statistical mechanics, as well as a variety of molecular

simulation techniques. Here, we expand on these ideas by introducing a granular potential into the Edwards ensemble, as an analogue to the chemical potential, and explore its properties using a simple model of a granular system.

The remainder of the paper is organized as follows: Section 2 provides a thermodynamic definition of the granular potential and its role in defining equilibrium in the Edwards ensemble. Section 3 describes the application of the granular potential to a simple model of a granular material, including a kinetic Monte Carlo simulation showing mass transport leading to equilibrium, and two analytical examples of equilibrium in systems able to exchange mass and volume. Our discussion and conclusions are contained in Sections 4 and 5, respectively.

2 A Granular Potential

The Edwards ensemble^{6,7} provides a starting point for a statistical mechanics of granular systems by defining an ensemble where all the jammed states of a system with the same volume, V , and a fixed number of particles, N , are equally probable. The probability of finding a given jammed state is then,

$$P_i = e^{-S/\lambda} \delta(V - W_i) \Theta, \quad (1)$$

where W_i is the Hamiltonian-type volume function for the configuration, S is the entropy, λ is the analog to the Boltzmann constant,

$$\Theta = \begin{cases} 1 & \text{if collectively jammed} \\ 0 & \text{otherwise} \end{cases}, \quad (2)$$

is the collective jamming condition and the normalization of the probability is given by,

$$e^{S/\lambda} = \int \delta(V - W_i) \Theta d(\text{all degrees of freedom}). \quad (3)$$

Integrating Eq. 3 and taking the natural log yields,

$$S/\lambda = \ln \Omega(V, N), \quad (4)$$

where $\Omega(V, N)$ is the number of collectively jammed configurations.

^a Department of Chemistry, University of Saskatchewan, Saskatoon, SK, S7N 0H1, Canada

^b Department of Physical and Computational Chemistry, Shahid Beheshti University, Tehran 19839-9411, Iran.

^c Centre for Quantum Topology and its Applications (quanTA), University of Saskatchewan, SK S7N 5E6, Canada. E-mail: richard.bowles@usask.ca

In conventional thermal statistical mechanics, the partition function is connected to the other thermodynamic parameters through the entropy and the first law, but there is no clear definition of heat and work for granular systems. Instead, we can write an analog to the thermodynamic fundamental equation, where the volume replaces the role of the energy, and introduce new granular thermodynamic potentials that affect variations of the volume, to give for example,

$$dV = X dS + \gamma dN. \quad (5)$$

Equation 5 defines Edwards compactivity for a system with fixed N ,

$$X = \left(\frac{\partial V}{\partial S} \right)_N, \quad (6)$$

as a granular equivalent to the thermal temperature that measures the capacity of the system to be compressed.

The second term on the right of the equality in Eq. 5 introduces the granular potential, γ , as the intensive conjugate variable to N that captures the effect of adding a particle to the system, as an analogy to the chemical potential. We can also use the fundamental equation to establish the key characteristics of the granular potential. For example, at constant volume, $dV = 0$, so Eq. 5 rearranges to give,

$$\left(\frac{\partial S}{\partial N} \right)_V = -\frac{\gamma}{X}. \quad (7)$$

At constant V , the insertion of a particle has two entropic affects. The entropy is an extensive quantity, so adding a particle necessarily increases S . However, the added particle also occupies volume, which increases the density of the system, reducing the number of accessible jammed states. The nature of the two contributions to the granular potential can be seen clearly by taking the derivative of Eq. 5 with respect to N at constant X , to obtain,

$$\frac{\gamma}{X} = \frac{1}{X} \left(\frac{\partial V}{\partial N} \right)_X - \left(\frac{\partial S}{\partial N} \right)_X, \quad (8)$$

where $(\partial V/\partial N) = V/N$ and $(\partial S/\partial N) = S/N$ are the partial molar volume and partial molar entropy, respectively, which become their molar quantities for a single component system.

The conditions for equilibrium in a conventional thermodynamic system are obtained by maximizing the total entropy, $S = S_1 + S_2$, of an isolated composite system, composed of two subsystems in contact with each other, that are able to exchange energy, mass and volume, subject to conservation conditions. We can do the same here. Writing Eq. 5 for subsystems 1 and 2 and using the conservation of mass, $dN = dn_1 + dn_2 = 0$, and volume, $dV = dV_1 + dV_2$, to obtain the variation of the total entropy,

$$dS = dS_1 + dS_2 = 0 \\ = \left(\frac{1}{X_1} - \frac{1}{X_2} \right) dV_1 - \left(\frac{\gamma_1}{X_1} - \frac{\gamma_2}{X_2} \right) dn_1. \quad (9)$$

Both n_1 and V_1 are independent, so Eq. 9 is only satisfied if the coefficients are zero. At constant n_1 the systems are in equilibrium when $X_1 = X_2$, at constant V the systems are at equilibrium when $\gamma_1/X_1 = \gamma_2/X_2$ and both equalities are required for general equilibrium.

3 Application to a Simple Model

To obtain a concrete understanding of the role the granular potential plays in equilibrium we study a simple model consisting of two-dimensional (2D) hard discs, with diameter σ , confined between hard walls separated by a distance $H/\sigma < 1 + \sqrt{3}/4$ (see Fig 1a). The model has been used previously to study the compactivity in granular systems¹⁶, as well as glassy relaxation¹⁷⁻²², because all of the jammed states can be fully characterized. Briefly, in 2D, a particle is locally jammed if it has three rigid contacts, not all located in the same semicircle, but the local jamming of all the particles is not sufficient for collective jamming²³ as the concerted motion of groups of particles can lead to unjamming. The restriction on H/σ prevents such rearrangements. It also ensures that discs can only touch their nearest neighbour on each side and the wall. As a result, there are only two local jamming environments, a dense structure with a volume $v_0 = H\sqrt{(2\sigma - H)H}$, formed when two discs are in contact across the channel, and a defect state with volume $v_1 = H\sigma$, formed when two discs are in contact along the channel. The total volume per particle of a jammed state is then given by,

$$V/N = (1 - \theta)v_0 + \theta v_1, \quad (10)$$

where $\theta = N_1/(N_0 + N_1)$ is the fraction of defects in the system, with N_0 and N_1 being the number of dense and defect states in the packing respectively, and $N_1 + N_0 = N$. The whole system remains collectively jammed as long as there are no neighbouring defects (see Fig. 1(a), adopting the most dense jammed state as $\theta \rightarrow 0$ and the least dense jammed state as $\theta \rightarrow 0.5$). The entropy of the system is also just a function of defect fraction¹⁷,

$$S(\theta)/\lambda N = (1 - \theta)\ln(1 - \theta) - (1 - 2\theta)\ln(1 - 2\theta) - \theta \ln \theta, \quad (11)$$

that exhibits a maximum when $\theta = 1/2 - \sqrt{5}/10$. Finally, all the packings of the system are isostatic and the model satisfies the Edwards postulate of equiprobable states.

The process of mass transport, leading to equilibrium, in our granular system can best be demonstrated using a simple simulation. We consider a system of $N = 2000$ discs and $H/\sigma = 1.86$, divided into two subsystems with volumes $V_1/\sigma^2 = 949.15$ and $V_2/\sigma^2 = 1167.75$, with $V = V_1 + V_2$, both initially containing $n_1(t = 0) = n_2(t = 0) = 1000$ particles. The particles in subsystem 1 are initially arranged in the most dense state, with no defects ($\theta_1 = 0$), while we randomly place defects in subsystem 2 such that there are no neighbouring defects and $\theta_2 = 0.24$. The location of the boundaries separating the two systems are fixed but particles can pass through. Granular systems need dynamics that takes them from jammed state to jammed state so they can sample the ensemble of states. Experimentally, this is usually achieved by shaking or tapping the system, but given all the jammed states are known, we use a simple kinetic Monte Carlo (KMC) scheme that takes the system directly between jammed states at fixed V and satisfies detailed balance (see Appendix for details). The simulation is run for 2000 time steps and average quantities are calculated over the last 1800 time steps.

As described, our composite system represents an isolated granular system with fixed total volume and total number of parti-

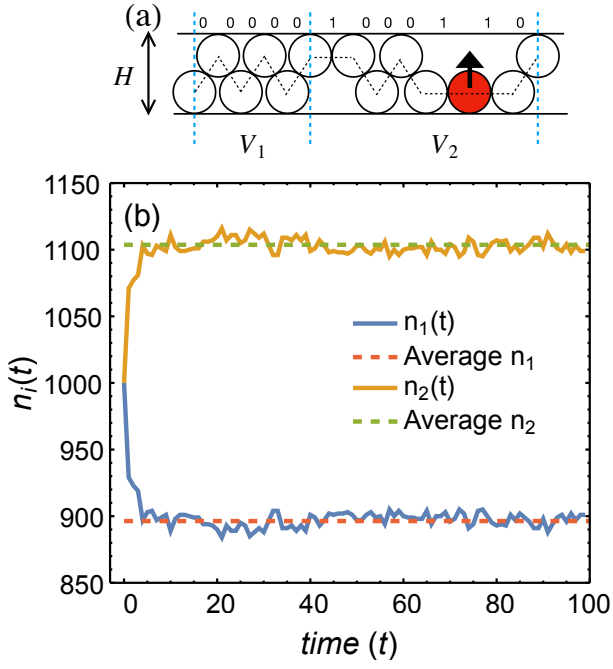


Fig. 1 (a) Granular model showing the dense (0) and defect (1) states. Neighbouring defects (11) allow the shaded (red) particle to become unjammed. The vertical dashed lines denote the subsystems with volumes, V_1 and V_2 . (b) The number of particles in each subsystem as a function of time (solid lines) compared to their averages (dashed lines).

cles. The two subsystems also have fixed volumes but are able to exchange particles, subject to the constraint $n_1 + n_2 = N$. Figure 1(b) shows the evolution of $n_i(t)$, the number of discs in each subsystem, as a function of time. Both subsystems start with same number of particles, but discs rapidly move from subsystem 1, where the density is high, into subsystem 2, until both $n_i(t)$ plateau and fluctuate around what is clearly their equilibrium values, $\langle n_1 \rangle = 896 \pm 5$ and $\langle n_2 \rangle = 1103 \pm 5$. The degree of confinement in the model explicitly prevents the particles from passing each other so they cannot diffuse. Instead, the defects diffuse through the system, with defect pairs sometimes annihilating and then spontaneously reforming in another part of the system in order to keep the total defect fraction constant and the system jammed. This leads to a redistribution of the volume and as the defects diffuse into V_1 , effectively expanding average volume per particle in this region, some particles are pushed from V_1 into V_2 , until equilibrium is obtained. In a molecular system, the transport of material between subsystems would be driven by differences in the chemical potential and the system would come to equilibrium when the chemical potential is the same in each system. The mass transport observed in our simulation suggests that a granular potential may serve a similar role.

The granular properties of our composite system can be obtained analytically as a function n_1 , using, Eqs. 10, 11, the conservation of mass and volume, along with Eqs. 6 and 8, where we have also used $(\partial V / \partial S)_N = (\partial V / \partial \theta)_N (\partial \theta / \partial S)_N$. Figure 2(a) shows the total entropy for the composite system exhibits a line of equivalent maxima corresponding to the equilibrium defined by Eq. 9. Figure 2(b) shows the entropy per particle for a system with the volume V_1 cor-

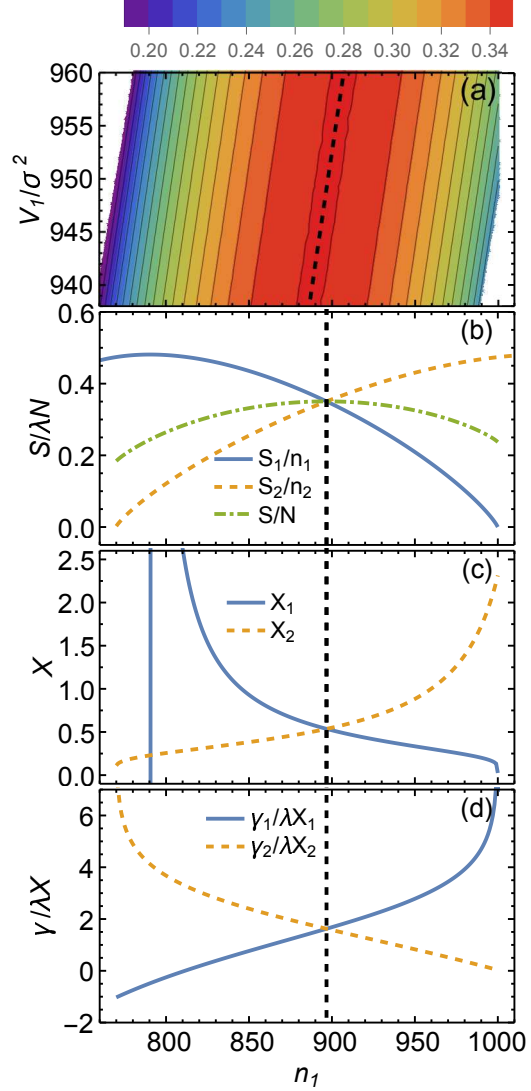


Fig. 2 (a) Contour plot of total entropy, S , as a function of n_1 and V_1 , with $V/\sigma^2 = 2116.9$, $N = 2000$ and $H_1/\sigma = H_2/\sigma = 1.86$. Dashed line indicates a ridge of equivalent maxima. (b) Entropy, (c) compactivity and (d) granular potential as a function of n_1 for the composite system with fixed $V_1/\sigma^2 = 949.15$ and $V_2/\sigma^2 = 1167.75$. Vertical black dashed lines denote the equilibrium value of n_1 .

responding to our simulation. The upper bound to n_1 occurs when subsystem 1 contains enough particles to be in the most dense jammed state, where $\theta_1 = 0$ and $S_1 = 0$. The lower bound to n_1 occurs when enough particles have moved into subsystem 2 to cause it to be in the most dense jammed state, where $\theta_2 = 0$ and $S_2 = 0$. The equilibrium value for $n_1 = 896.7$, obtained as the maximum in entropy of the isolated composite system, $S = S_1 + S_2$, is the same as that obtained in the simulation. The compactivity in subsystem 1 (Fig. 2(c)) increases as n_1 decreases, and actually diverges when S_1 goes through its maximum. The divergence point appears as the vertical line in X_1 . At smaller n_1 , the number of jammed states in the system begins to decrease and the compactivity becomes negative, which is analogous to the appearance of negative temperatures in thermal systems with similar distributions in their density of states. At the same time, X_2 decreases with decreasing n_1 and $X_1 = X_2$ at equilibrium. Figure 2(d) shows γ_1/X_1 decreases, and γ_2/X_2 increases, as particles move from subsystem 1 to subsystem 2, and $\gamma_1/X_1 = \gamma_2/X_2$ at equilibrium. This confirms that mass, in a granular system, moves from regions of high γ/X to regions of low γ/X . If we choose a different V_1 , the maximum occurs at a different n_1 along the dashed line, but the equilibrium values of X and γ/X remain the same because the compactivity and granular potential should be uniform throughout the system and independent of where we choose the dividing surface for subsystems.

To test the generality of our result, we build a second composite system with $H_1/\sigma = 1.86$ and $H_2/\sigma = 1.70$, so the particles in the different height channels occupy different volumes when they are in the two allowed local jamming environments. This example is equivalent to allowing molecular exchange between two systems with distinct chemical environments, where we would still expect the chemical potential in the systems to be equal at equilibrium. Figure 3(a) shows that the composite system exhibits a single maximum, despite the near parallel appearance of the contour lines, corresponding to the coexistence between the two subsystems. However, the equilibrium is located at the point where both subsystems have reached their maximum in entropy (See Fig. 3(b)) so we find $X_1 = X_2 = \infty$ and $\gamma_1/X_1 = \gamma_2/X_2 \approx -0.4812$, which is minus the entropy per particle at the maximum of the entropy maximum and is consistent with the expectations of Eq. 8 at $X = \infty$. We can also consider equilibrium in the composite system where volumes V_1 and V_2 are fixed. For example, Fig. 4 shows the thermodynamics of the composite system with V_1 fixed away from the global equilibrium. At the maximum $S \approx 0.3916$, which is lower than the global maximum as expected, and $S_1 \neq S_2$. As a result, we still find that $\gamma_1/X_1 = \gamma_2/X_2$, but since $dV_1 = 0$, the equality of compactivities in Eq. 9 is no longer required, and $X_1 \neq X_2$.

The granular potential gives us insight into the effects of adding a particle to a jammed system, but it is important to recognize that particle insertion in a granular system is fundamentally different from that in a chemical system. The particles in the initial jammed state must rearrange to accommodate the new particle and ensure the final state is also jammed, which is not the case, for example, in the Widom insertion method²⁴ used to calculate the chemical potential. This has consequences for the effects of adding a particle to the system. Figure 5 plots γ/X as a function of the compactivity, along with its two thermodynamic contributions identified in

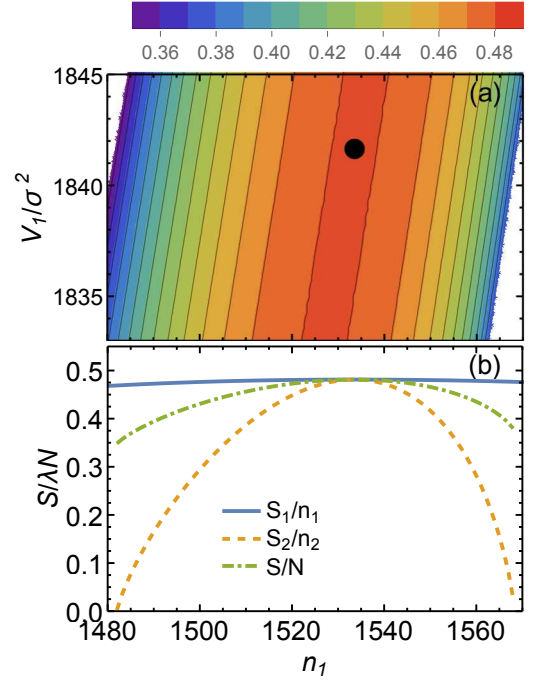


Fig. 3 (a) Contour plot of total entropy, S , as a function of n_1 and V_1 , with $V_1/\sigma^2 = 2470.58$, $N = 2000$, $H_1/\sigma = 1.86$ and $H_2/\sigma = 1.7$. Black point indicates maximum. (b) Entropy for system with $V_1/\sigma^2 = 1841.64$ corresponding to equilibrium.

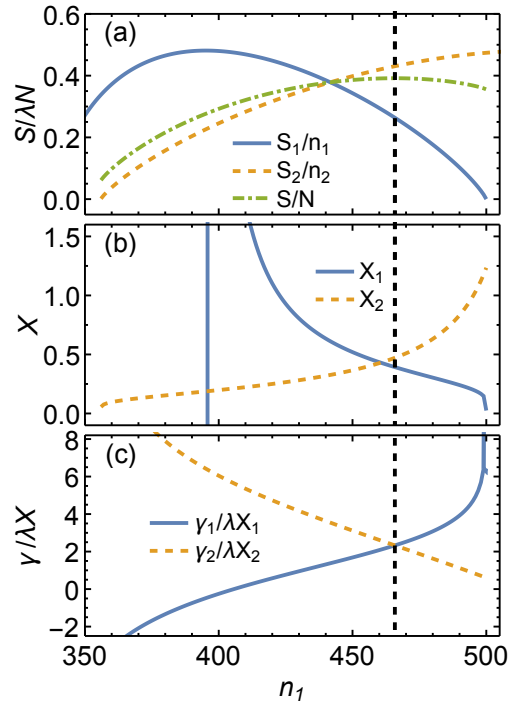


Fig. 4 (a) Entropy, (b) compactivity and (c) granular potential as a function of n_1 for a composite system with $N = 2000$, $H_1/\sigma = 1.86$, $H_2/\sigma = 1.70$, $V_1/\sigma^2 = 465.83$ and $V_2/\sigma^2 = 1996.01$. Vertical black dashed line denotes the equilibrium value of n_1 .

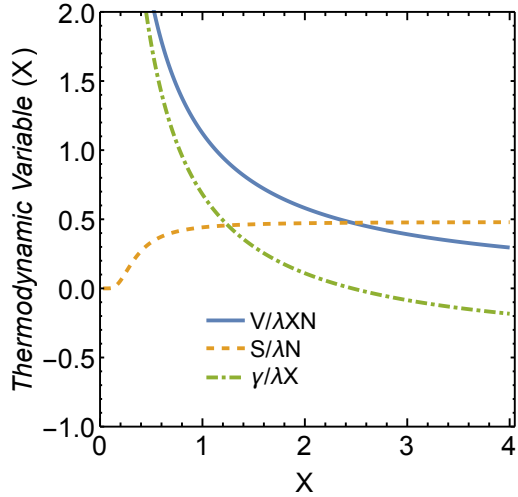


Fig. 5 Thermodynamic contributions to γ/X from Eq. 8 as function of compactivity, for a system $H/\sigma = 1.86$.

Eq. 8. At high X , there are a large number of expanded jammed states, so the entropic term makes a large contribution, while the volume term, scaled by the compactivity, is small. The resulting value for γ/X (with $X > 0$) is negative, which implies that adding a particle to the system at constant volume increases the entropy (Eq. 7). However, as X decreases, the volume term begins to increase because jammed states are more compact and the system needs to eliminate more defect states in order to accommodate the new particle. At the same time S/N is decreasing, so eventually γ/X changes sign, indicating the addition of a particle to the system will lead to a decrease in the entropy.

4 Discussion

The key result of our work has been to rigorously establish the properties of a granular potential for a model that is known to satisfy the Edwards postulate. In particular, we find that at constant volume, mass moves from high to low γ/X , until equilibrium is reached, in analogy to the chemical potential in molecular systems. In addition, Eq 8 identifies the need for partial molar volumes and entropies that again have analogous functions to those observed in molecular systems, and play important roles in our understanding of mixtures. Chang et al²⁵ recently took a step in this direction, using partial molar volumes and activity coefficients to describe jamming densities in bi-dispersed granular packings, and Lui et al²⁶ suggest that a granular granular potential needs to be developed to understand binary mixtures of confined discs.

The granular potential will also play an important role in understanding phase equilibria in granular materials, where we expect both the compactivity and granular potentials to be equal in both phases at coexistence. For example, hard sphere packings appear to exhibit a first order freezing transition near random close packing from the amorphous packing to the face centred crystal^{27–29}, as do sheared granular systems^{30,31}, and orientational ordering has been observed in the packings of cylindrical granular particles³².

Our example of equilibrium involving discs confined to two channels with different heights provides a limiting case for such

a phase transition. The particles in the narrower channel occupy more space than those in the wider channel, even though they have the same two types of local packing environments, which gives rise to different volume distributions for the jammed packings in each channel. This mimics the distinct distributions we would expect to see in two phases of a granular system in higher dimensions. The coexistence in our model system occurs at $X = \infty$ because both distributions have the same entropy maximum, just located at different volumes, which gives $\Delta S = S_1 - S_2 = 0$ and $\Delta V = V_1 - V_2 > 0$. However, in general, we would expect the high density phase of any two phase granular system to have a smaller number of jammed states and a lower entropy, which would move the coexistence point to lower X and the transition would become first order with $\Delta S > 0$ and $\Delta V > 0$.

However, work is still required to put the granular potential on the same fundamental footing as the chemical potential. Our current analysis relies on the validity of the Edwards postulate for the equiprobability of jammed states with the same volume. This is true in our model, and recent simulations suggest it is also true for jammed hard spheres near the jamming point¹⁴, but it does not appear to be generally valid¹². We will need to examine the role of the granular potential in other ensembles, such as the stress ensemble^{11,33}. There is also no simple way to measure the granular potential. Eq. 8 shows that γ/X can be obtained from the equation of state and entropy of the material, but it is not immediately obvious that a Widom particle insertion type analysis can be developed because of the global nature of the jamming constraint.

5 Conclusions

To conclude, we have shown that mass transport towards equilibrium in a simple model of a granular system is driven by differences in the ratio of the granular potential to the compactivity, and that the system comes to equilibrium when both the compactivity and the granular potential are uniform. The model also shows that the granular potential plays a role in determining the equilibrium between systems with different packing distributions, as we would expect in a phase transition, suggesting that the granular potential may be a useful concept in understanding a broad range of granular phenomena.

Author Contributions

All authors contributed equally to this work.

Conflicts of interest

There are no conflicts to declare.

Acknowledgements

We would like to acknowledge NSERC grant RGPIN–2019–03970 (R. K. B) for financial support. Computational resources and support were provided by the Prairie DRI Group and the Digital Research Alliance of Canada.

Appendix

This appendix describes the kinetic Monte Carlo Scheme used in our simulations. The state of the system can be characterized as a spin model, assigning particles in the most dense and defect states

a 0 or 1 respectively. A single KMC move involves randomly selecting a particle and randomly swapping its local environment with the particle to the left or right. For example, $\{10\} \rightarrow \{01\}$ effectively moves a defect to the right, while a swap $\{00\} \rightarrow \{00\}$ has no net effect on the state. If the move results in a stable configuration, with no neighbouring defects, the move is accepted.

If the move generates an unstable environment, the defect pair is eliminated ($\{11\} \rightarrow \{00\}$). However, the total number of defects must remain fixed to ensure the system stays jammed at constant V . A defect pair is then inserted by randomly selecting a particle. If it is a zero, then an attempt is made to insert a second defect two sites to the left or right with equal probability, ($\{00000\} \rightarrow \{01010\}$). If a stable configuration is created, then the move is accepted, otherwise it is rejected. This is repeated until two defects are successfully inserted, returning the number of defects to its original value. One unit of time in the simulation corresponds to N KMC moves.

Notes and references

- 1 E. R. Nowak, J. B. Knight, E. Ben-Naim, H. M. Jaeger and S. R. Nagel, *Phys. Rev. E*, 1998, **57**, 1971–1982.
- 2 J. Brujić, P. Wang, C. Song, D. L. Johnson, O. Sindt and H. A. Makse, *Phys. Rev. Lett.*, 2005, **95**, 128001.
- 3 P. Philippe and D. Bideau, *Europhys. Lett.*, 2002, **60**, 677–683.
- 4 P. M. Reis, R. A. Ingale and M. D. Shattuck, *Phys. Rev. Lett.*, 2007, **98**, 188301.
- 5 B. Kou, Y. Cao, J. Li, C. Xia, Z. Li, H. Dong, A. Zhang, J. Zhang, W. Kob and Y. Wang, *Nature*, 2017, **551**, 360–363.
- 6 S. Edwards and R. Oakeshott, *Phys. A: Stat. Mech. Appl.*, 1989, **157**, 1080–1090.
- 7 S. F. Edwards and D. V. Grinev, *Phys. Rev. E*, 1998, **58**, 4758–4762.
- 8 S. Edwards, *Phys. A: Stat. Mech. Appl.*, 2005, **353**, 114–118.
- 9 G.-J. Gao, J. Blawdziewicz, C. S. O’Hern and M. Shattuck, *Phys. Rev. E*, 2009, **80**, 061304.
- 10 K. Wang, C. Song, P. Wang and H. A. Makse, *Phys. Rev. E*, 2012, **86**, 011305.
- 11 R. Blumenfeld, J. F. Jordan and S. F. Edwards, *Phys. Rev. Lett.*, 2012, **109**, 238001.
- 12 J. G. Puckett and K. E. Daniels, *Phys. Rev. Lett.*, 2013, **110**, 058001.
- 13 D. Bi, S. Henkes, K. E. Daniels and B. Chakraborty, *Annu. Rev. Condens. Matter Phys.*, 2015, **6**, 63–83.
- 14 S. Martiniani, K. J. Schrenk, K. Ramola, B. Chakraborty and D. Frenkel, *Nat. Phys.*, 2017, **13**, 848–851.
- 15 A. Baule, F. Morone, H. J. Herrmann and H. A. Makse, *Rev. Mod. Phys.*, 2018, **90**, 015006.
- 16 R. K. Bowles and S. S. Ashwin, *Phys. Rev. E*, 2011, **83**, 031302.
- 17 R. K. Bowles and I. Saika-Voivod, *Phys. Rev. E*, 2006, **73**, 011503.
- 18 M. Z. Yamchi, S. S. Ashwin and R. K. Bowles, *Phys. Rev. Lett.*, 2012, **109**, 225701.
- 19 S. S. Ashwin, M. Z. Yamchi and R. K. Bowles, *Phys. Rev. Lett.*, 2013, **110**, 145701.
- 20 M. J. Godfrey and M. A. Moore, *Phys. Rev. E*, 2014, **89**, 032111.
- 21 M. Z. Yamchi, S. S. Ashwin and R. K. Bowles, *Phys. Rev. E*, 2015, **91**, 022301.
- 22 M. J. Godfrey and M. A. Moore, *Phys. Rev. Lett.*, 2018, **121**, 075503.
- 23 S. Torquato and F. H. Stillinger, *J. Phys. Chem. B*, 2001, **105**, 11849–11853.
- 24 D. Frenkel and B. Smit, *Academic Press, New York*, 2002.
- 25 C. S. Chang and Y. Deng, *Granul Matter*, 2022, **24**, 58.
- 26 D. Liu and G. Müller, *Phys. Rev. E*, 2022, **105**, 024904.
- 27 Y. Jin and H. A. Makse, *Phys. A: Stat. Mech. Appl.*, 2010, **389**, 5362–5379.
- 28 M. Hanifpour, N. Francois, S. M. V. Allaei, T. Senden and M. Saadatfar, *Phys. Rev. Lett.*, 2014, **113**, 148001.
- 29 M. Hanifpour, N. Francois, V. Robins, A. Kingston, S. M. V. Allaei and M. Saadatfar, *Phys. Rev. E*, 2015, **91**, 062202.
- 30 F. Rietz, C. Radin, H. L. Swinney and M. Schröter, *Phys. Rev. Lett.*, 2018, **120**, 055701.
- 31 W. Jin, C. S. O’Hern, C. Radin, M. D. Shattuck and H. L. Swinney, *Phys. Rev. Lett.*, 2020, **125**, 258003.
- 32 Y. Ding, D. Gong, J. Yang, Z. Xu, Z. Wang, J. Li, B. Hu and C. Xia, *Soft Matter*, 2021, **18**, 726–734.
- 33 E. S. Bililign, J. E. Kollmer and K. E. Daniels, *Phys. Rev. Lett.*, 2019, **122**, 038001.